Geometric optimal techniques to control the muscular force response to functional electrical stimulation using a non-isometric force-fatigue model

Bernard Bonnard, Jérémy Rouot

▶ **To cite this version:**

Bernard Bonnard, Jérémy Rouot. Geometric optimal techniques to control the muscular force response to functional electrical stimulation using a non-isometric force-fatigue model. Journal of Geometric Mechanics, 2021, 13 (1), pp.1-23. 10.3934/jgm.2020032 . hal-02611095v2

HAL Id: hal-02611095
https://inria.hal.science/hal-02611095v2

Submitted on 1 Sep 2020

HAL is a multi-disciplinary open access archive for the deposit and dissemination of scientific research documents, whether they are published or not. The documents may come from teaching and research institutions in France or abroad, or from public or private research centers.

L'archive ouverte pluridisciplinaire **HAL**, est destinée au dépôt et à la diffusion de documents scientifiques de niveau recherche, publiés ou non, émanant des établissements d'enseignement et de recherche français ou étrangers, des laboratoires publics ou privés.

Volume **X**, Number **0X**, XX **200X** pp. **X–XX**

GEOMETRIC OPTIMAL TECHNIQUES TO CONTROL THE MUSCULAR FORCE RESPONSE TO FUNCTIONAL ELECTRICAL STIMULATION USING A NON-ISOMETRIC FORCE-FATIGUE MODEL

Bernard Bonnard

McTAO team, INRIA Sophia Antipolis
2004 Route des Lucioles, 06902 Valbonne, France

Jérémy Rouot *

McTAO team, INRIA Sophia Antipolis
2004 Route des Lucioles, 06902 Valbonne, France

(Communicated by the associate editor name)

Abstract. A recent force-fatigue parameterized mathematical model, based on the seminal contributions of V. Hill to describe muscular activity, allows to predict the muscular force response to external electrical stimulation (FES) and it opens the road to optimize the FES-input to maximize the force response to a pulse train, to track a reference force while minimizing the fatigue for a sequence of pulse trains or to follow a reference joint angle trajectory to produce motion in the non-isometric case. In this article, we introduce the geometric frame to analyze the dynamics and we present Pontryagin types necessary optimality conditions adapted to digital controls, used in the experiments, vs permanent control and which fits in the optimal sampled-data control frame. This leads to Hamiltonian differential variational inequalities, which can be numerically implemented vs direct optimization schemes.

1 Introduction

The mathematical force-fatigue models of external electrical stimulations (FES) aim to predict the muscular response and, in the so-called non-isometric case, to produce a joint angle trajectory. They can be used to muscular reinforcement, rehabilitation or to produce motion in biomechanics, in the case of paralysis, which is an important long-term medical purpose.

Historically, a first model called in this article the *Hill-Huxley model* [21] is a consequence of life-lasting work by V. Hill to analyze the muscular activity and whose earliest work in this domain was awarded by 1922 Nobel prize of medicine. In this model, the force response is roughly given by a non-linear second order differential equation, which describes the *electric conduction* and includes the phenomenon of

2010 *Mathematics Subject Classification.* 49K15, 93B07, 92B05.

Key words and phrases. Biomechanics force-fatigue models, Geometric optimal control, Sampled-data control problem, Pontryagin type necessary conditions, Hamiltonian differential variational inequality.

This research paper benefited from the support of the FMJH Program PGMO and from the support of EDF, Thales, Orange and the authors are partially supported by the Labex AMIES.

* Corresponding author: J. Rouot.

tetania and can be interpreted as the memory effect of two successive pulses. A second more recent step led to models taking into account the dynamics of the *fatigue variables*, see for instance the *Ding et al. models* [16, 17, 18] in the *isometric case*, that is without joint angular motion. They were very recently generalized to provide the so-called *Marion et al. model*, analyzed in this article, where the parameters associated to several stimulation protocols are validated experimentally and reported in the references [27, 28]. They are given in Table 2 and used in our numeric simulations. This model has to catch the features of the nonlinear dynamics and has to be robust to make the optimal control analysis. It contains the second-order Hill-Huxley model, with one time scale related to electrical conduction, which drives the force response to FES-input, and the evolution of three *fatigue variables* with a different time scale, which are driven by the force and the dynamics of the angular joint variable. A *nonlinear pendulum* is used to describe the response of the joint variable driven by internal biomechanics forces and the muscular force response to FES-input. Besides, it contains many coupling parameters which have to be identified in relation with the stimulation protocols.

In fine, this will lead in the future to *adaptative optimization algorithms*, see [15, 2] for preliminary results in this direction in the isometric case. In this article, we concentrate to *(open loop) optimal control* in relation with the problem of maximizing the force response to a single pulse train or to produce a reference force for a sequence of stimulation trains, this is the case for the non-isometric Marion et al. model. Our aim is to generalize preliminary optimal control results in the isometric case, see [3, 4, 5].

The geometric frame is well-adapted, since the FES-input corresponds to *constant control* over each interval $[t_i, t_{i+1}]$, where t_i are the stimulation times. A *digital constraint* is imposed by the FES-input and over a single train of length T, only a *fixed* bounded number of pulses can be applied, with a *minimal digital bound* $t_{i+1} - t_i \geq I_m > 0$ on the interpulse. In this context, the fine controllability properties of the system are related to *Lie algebraic computations* in the area of geometric control developed at the end of 70's, see for instance [31, 23, 13, 24] concerning controllability, observability, feedback invariance and input-output properties.

The various control protocols lead to *Mayer* optimal control problems. Due to digital control, the control set is *finite dimensional* and the optimal control problems can be handled using a *direct scheme*, where optimization algorithms can be used with a further state-space discretization. Another approach being an *indirect scheme* based on *Pontryagin type necessary conditions* restricting to sampled-data control. More specifically we can refer to [11, 12], adapted in [3] to deal with the FES-input and applied to the isometric case. Note that, from a more general viewpoint, sampled-data optimal control is related to compute specific (Gâteaux) types derivatives, and is in the historical continuity of the *classical calculus of variations* [6, 20] vs Pontryagin et al. maximum principle standard case, using a *single* type of L^1-*variations* and leading to necessary optimality conditions applicable to many very practical problems [26, 30].

One aim of this article is to relate both approaches, standard case vs sampled-data case, in relation with the specific Mayer problems concerning Marion et al. model. Moreover, in the sampled-case, due to control constraints on the amplitudes and on the interpulses, this gives *Hamiltonian differential variational inequalities*, which have to be handled with numerical schemes.

Note that in the standard case the recent techniques in geometric optimal control developed at the end of the 90's [1, 8, 9] and in the specific case of *single-input* systems the concept of regular synthesis boils down to bound the number of switches of bang-singular arcs of an optimal policy using again *Lie brackets computations*. In the sampled-data case, if the number of switches is uniformly bounded by definition, the optimality conditions are not very useful at present to determine the optimal subcases saturating the interpulse or the amplitude in the optimization protocol. Hence the *numeric* simulations are a more crucial tool.

The contribution and organization of this article are the following. In section 2, we present the Marion et al. model [28] as a generalization of the Hill-Huxley model [21] and the Ding et al. model [16] and introduce the related Mayer optimal control problems. Preliminary properties of the dynamics are given and sensitivity analysis with respect to parameters leading to model reduction is defined in an Hamiltonian frame convenient for numerical simulations, presented at the end of the section and concerning the Ding et al. model. In section 3, we introduce the geometric frame (Lie algebraic computations) to analyze the controllability of the Marion et al. model. Singular trajectories are defined and computed in the model (note that they are absent in the Ding et al. model). In section 4, Pontryagin's type techniques in the permanent vs the sampled-data case, based on [11, 12], are discussed in the case of Mayer problems and have to be adapted in our specific study. This leads to necessary optimality conditions in the form of Hamiltonian differential variational inequalities. Finally, in section 5, we present first algorithms to solve the optimization problems based on a direct and an indirect methods. Second we present preliminary numeric simulations, comparing our indirect optimization scheme with a direct scheme and concerning the isometric case, where the cost function amounts to maximize the force response vs the non-isometric case, where the final cost takes into account the *fatigue variables*.

2 The non-isometric Marion et al. model. Basic properties of the dynamics and related optimal control problems. Sensitivity analysis

The complete model is presented in the historical context of three steps to construct a complex final model.

2.1 The Hill-Huxley model, the FES-input and the phenomenon of tetania

First of all, the (physical) input associated to external electrical stimulation is a sequence of *pulse trains*, with *rest periods*, each train of length T is mathematically given by a set of *Dirac pulses*

$$v(t) = \sum_{i=0}^{n} \eta_i \, \delta(t - t_i),$$

where $\eta_i \in [0, 1]$ are the normalized amplitudes, $0 = t_0 < t_1 < \cdots < t_n < T$ represent the impulse times and $I_i = t_i - t_{i-1}$, $i = 1, \ldots, n$ are the *interpulses*. By convenience, one takes $t_{-1} = -\infty$ and $t_{n+1} = T$. Due to digital control, over one stimulation train, the number of sampling times n is fixed and we have a minimal impulses restriction $I_i \geq I_m > 0$ for $i = 1, \ldots, n$.

Second, one must introduce the concept of *FES-input* and the *phenomenon of tetania*. The FES-input, denoted by $E_s(t)$ and used in this article as the sampled-data control driving the force response, is related to $v(\cdot)$ using a RL-electrical dynamics and is given on $[0,T]$ by

$$\dot{E}_s(t) + \frac{E_s(t)}{\tau_c} = \frac{1}{\tau_c}\sum_{i=0}^{n} \eta_i \delta(t-t_i) R_i \tag{1}$$

with $E_s(0) = 0$, τ_c is a time scale related to electrical conduction and R_i is a parameter describing the phenomenon of tetania defined by

$$R_i = \begin{cases} 1 & \text{if } i = 1 \\ 1 + (R_0 - 1)\, e^{-\frac{t_i - t_{i-1}}{\tau_c}} & \text{if } i > 1 \end{cases}, \tag{2}$$

where $R_0 > 1$ is a constant. Note that if $t_i - t_{i-1} \gg 1$, we have $R_i \simeq 1$ while if $t_i - t_{i-1} \ll 1$, $R_i \simeq R_0$. More complicated models can be used where R_0 depends upon the fatigue and our analysis can be generalized to this case.

Integrating the linear dynamics, the FES-input is given by

$$E_s(t) = \frac{e^{-1/\tau_c}}{\tau_c} \sum_{i=0}^{n} R_i e^{t_i/\tau_c} \eta_i H(t-t_i), \tag{3}$$

where $H(t-t_i)$ denotes the *Heaviside step function*.

Definition 2.1. Once the sampling times are fixed, the sum $\sum_{i=0}^{n} R_i e^{t_i/\tau_c} \eta_i H(t-t_i)$ over a train of length T is a superposition of constant controls u_i on $[t_i, T]$ and leads to a *sampled-data control problem*, each control being represented as the sequence $\delta = (\eta_0, \eta_1, \ldots, \eta_n, t_1, \ldots, t_n) \in \mathbb{R}^{2n+1}$.

The third step in the model is to describe the biological *electrical conduction* due to (ionic) Ca^{2+}-concentration denoted C_N and whose variation is described by the linear dynamics

$$\dot{C}_N(t) + \frac{C_N(t)}{\tau_c} = E_s(t) \text{ for } t \in [0,T] \tag{4}$$

with $C_N(0) = 0$. Integrating the (resonant) system gives the following.

Lemma 2.2. *The Ca^{2+} concentration over a train of length T is given by*

$$C_N(t) = \frac{1}{\tau_c} \sum_{i=0}^{n} R_i e^{-\frac{t-t_i}{\tau_c}} \eta_i (t-t_i) H(t-t_i) \text{ for all } t \in [0,T]. \tag{5}$$

The final step in the model is to describe the force response described by the dynamics

$$\dot{F}(t) = -m_2(t)\, F(t) + m_1(t)\, A, \tag{6}$$

where m_1, m_2 are related to the *Michaelis-Menten model (1913)* in correspondence with the Hill dynamics and are given by

$$m_1(t) = \frac{C_N(t)}{K_m + C_N(t)}, \qquad m_2(t) = \frac{1}{\tau_1 + \tau_2\, m_1(t)}. \tag{7}$$

In those equations A, K_m, τ_1, τ_2 are fatigue parameters, A being a scaling parameters and K_m is interpreted as the Michaelis-Menten constant.

Definition 2.3. The dynamics (4),(6) describes the force-response to the FES-input and is called the *Hill-Huxley model*.

This dynamics can be integrated and we have the following proposition.

Proposition 1. *The Hill-Huxley model can be integrated by quadrature, using a time reparameterization.*

Proof. While C_N is given by (5), the force equation (6) is written as $\frac{\mathrm{d}F}{\mathrm{d}s} = m_3 - F$ with $\mathrm{d}s = m_2(t)\mathrm{d}t$, $m_3 = Am_1/m_2$. To integrate, use Lagrange formula. □

2.2 Isometric case: Ding et al. force-fatigue model

This model, based on a series of articles, see for instance [17], is constructed as follows. In the force model described by (6),(7), the fatigue parameters are assumed to satisfy a linear system driven by the force F of the form

$$\begin{cases} \dot{A}(t) = -\frac{A(t)-A_{rest}}{\tau_{fat}} + \alpha_A F(t) \\ \dot{K}_m(t) = -\frac{K_m(t)-K_{m,rest}}{\tau_{fat}} + \alpha_{K_m} F(t) \\ \dot{\tau}_1(t) = -\frac{\tau_1(t)-\tau_{1,rest}}{\tau_{fat}} + \alpha_{\tau_1} F(t), \end{cases} \tag{8}$$

depending upon an additional *single time scale* τ_{fat}, where $\alpha = (\alpha_A, \alpha_{K_m}, \alpha_{\tau_1})^\intercal$ are parameters and $(A_{rest}, K_{m,rest}, \tau_{1,rest})$ is the unique equilibrium point of the system with $F = 0$.

Definition 2.4. The dynamics (4),(6) coupled by (8) is an extension of the Hill-Huxley model and is called the *Ding et al. (isometric) force-fatigue model.*

Due to the single time scale τ_{fat}, the following is clear.

Proposition 2. *The linear system* (8) *driven by the force-control is not controllable and the fixed-time accessibility set is one-dimensional.*

2.3 The Marion et al. non-isometric force-fatigue model

A final model extension of the previous models is derived up to some simplifications of [28]. To our knowledge, it is the only model validated experimentally, where parameters can be identified using electrical stimulation protocols and typical parameters values are reported in Table 2,1. The model is constructed as follows.

$$\dot{F}(t) = m_1(t)\,(G(t) + A(t)) - m_2(t)\,F(t) \tag{9}$$

with m_1, m_2 being defined by (7) and where (A, G) are fatigue variables defined by

$$\begin{aligned} A(t) &= A_{90}(t)\left[a(90-\theta(t))^2 + b(90-\theta(t)) + 1\right] \\ G(t) &= v_1\theta(t)e^{-v_2\theta(t)}\dot{\theta}(t), \end{aligned} \tag{10}$$

where θ is the joint angular variable (the leg in the experimental protocol) with rest position at $\theta = 90°$ and the θ-dynamics is given by a nonlinear pendulum to describe large θ-evolution

$$\ddot{\theta}(t) = \frac{L}{I}(F_{ext}\cos\theta(t) - F(t)), \tag{11}$$

where $\ell = L/I$ is a torque parameter, $F_{ext} = F_{load} + F_M$ being the *external force* with F_{load} is the applied ankle weight, F_M is the resistance to the body and F is the muscular force response.

The fatigue variables satisfy the modified dynamics

$$\begin{aligned}
\dot{A}_{90}(t) &= -\frac{A_{90}(t) - A_{90,rest}}{\tau_{fat}} + (\alpha_{90} + \beta_{90}\dot{\theta}(t))\, F(t) \\
\dot{K}_m(t) &= -\frac{K_m(t) - K_{m,rest}}{\tau_{fat}} + (\alpha_{K_m} + \beta_{K_m}\dot{\theta}(t))\, F(t) \\
\dot{\tau}_1(t) &= -\frac{\tau_1(t) - \tau_{1,rest}}{\tau_{fat}} + (\alpha_{\tau_1} + \beta_{\tau_1}\dot{\theta}(t))\, F(t).
\end{aligned} \tag{12}$$

This model introduces new non-isometric parameters: (a, b, v_1, v_2) in (10) and $\beta = (\beta_{90}, \beta_{K_m}, \beta_{\tau_1})^\intercal$, which are the coupling parameters between the fatigue variables and the θ-dynamics.

Definition 2.5. The previous model, where (4) drives the Ca^{2+}-concentration C_N, is controlled by the FES-input and (9)-(12) drive the evolution of the force-fatigue variables, is called *the Marion et al. (non-isometric model).*

Parameters of the models Parameters depend on the individual, the specific load and the stimulation parameters. Identification of those parameters are an important experimental issue. Typical values are reported in Table 1,2 to make sensitivity analysis for model reduction and to perform numerical simulations to compute optimized pulse trains.

2.4 Mathematical representation of the equations

For mathematical analysis, the set of equations associated to the Marion et al. model is written in the following form.

The state variables are denoted as $x = (x_1, x_2, x_3, x_4, x_5, x_6, x_7)^\intercal = (C_N, F, \theta, \dot{\theta}, A_{90}, K_m, \tau_1)^\intercal$ and to deal with time dependence we use the notation

$$x_0(t) = \frac{1}{\tau_c} e^{-t/\tau_c}. \tag{13}$$

We substitute $u(t)$ to the FES-input and the system identified to (F_0, F_1) is written as

$$\dot{x}(t) = F_0(x(t)) + u(t)\, F_1(x(t)) \tag{14}$$

with $F_1(x) = e_1 = (1, 0, \ldots, 0)^\intercal$ and introducing the two time scales

$$\lambda_1 = -\frac{1}{\tau_c}, \quad \lambda_2 = -\frac{1}{\tau_{fat}}, \tag{15}$$

the F_0-dynamics is excerpted from the equations

$$\begin{aligned}
\dot{x}_1(t) &= \lambda_1 x_1(t) + u(t) \\
\dot{x}_2(t) &= \sigma(x_3(t), x_4(t), x_5(t))\, m_1(x_1(t), x_6(t)) - m_2(x_1(t), x_6(t), x_7(t))\, x_2(t) \\
\dot{x}_3(t) &= x_4(t) \\
\dot{x}_4(t) &= \ell(F_{ext} \cos x_3(t) - x_2(t))
\end{aligned} \tag{16}$$

with $\sigma = G + A$, coupled with the linear dynamics of the fatigue variables written as

$$\dot{\bar{x}}(t) = \lambda_2 \mathrm{Id}_3(\bar{x}(t) - \bar{x}^0) + (\alpha + \beta x_4(t))\, x_2(t) \tag{17}$$

with $\bar{x} = (x_5, x_6, x_7)$, $\bar{x}^0$ is the equilibrium point, Id_3 is the 3×3 identity matrix and α, β are fatigue vectors parameters.

The system is *an affine control system* (that is linear with respect to u) and note that F_1 reduces to $\frac{\partial}{\partial x_1}$.

2.5 Optimal control problem

Consider the smooth control system $\dot{x} = F(x,u)$ on $\mathbb{R}^n$ described by (F_0, F_1). A *Mayer problem* is a problem of the form $\min_{u\in\mathcal{U}} \varphi(x(T))$ where $\mathcal{U}$ is the set of admissible controls, φ is a (smooth) map from $\mathbb{R}^n$ and T is a fixed time. A *Lagrange problem* is a problem of the form $\min\limits_{u\in\mathcal{U}} \varphi(x(T)) + \int_0^T L(x,u)\mathrm{d}t$, where L is a (smooth) map called the Lagrangian. Extending the dynamics, one can restrict to the first case.

In particular in our study, we can consider the following problems:

- **(OC1):** Maximize the force response $x_2(T)$ at the end of a single pulse train.
- **(OC2):** Maximize a criterion taking into account force response or a fatigue variable x_i written as $\max\limits_{u(\cdot)} w_1 x_2(T) + w_2 x_i(T)$, with weights $w_1 > 0$, $w_2 > 0$, $i \in \{5,6,7\}$.
- **(OC3):** Reach a reference force F_{ref} and minimize the fatigue variables, over a long stimulation period (this problem will not be analyzed in this article).

2.6 Sensitivity analysis of the force response to the parameters

Since the dynamics is complex, a *model reduction* can be crucial for numeric purpose and we introduce the following approach to study the dynamics of the force response with respect to parameters or fatigue variables vs numeric approach [2]. This approach is fitted in an *Hamiltonian frame* and can be numerically handled using the *Hampath software* [14].

Definition 2.6. Consider a smooth *control system* of $\mathbb{R}^n$, $x \in \mathbb{R}^n$, $u \in \mathbb{R}^m$ being the control. The *Hamiltonian lift* is the function $H(z,u) = p \cdot F(x,u)$, where $p \in \mathbb{R}^n$ is the *adjoint vector* and $\cdot$ is the standard scalar product and $z = (x,p)$. If $H(z)$ is an Hamiltonian, we note $\vec{H}$ the associated vector field $(\partial H/\partial p, -\partial H/\partial x)^\intercal$. The *Poisson bracket* between two Hamiltonian functions is defined by $\{H_1, H_2\}(z) = \mathrm{d}H_1(\vec{H_2})(z)$.

Definition 2.7. Let $H(z)$ be a smooth Hamiltonian and take $z(\cdot)$ a smooth *reference trajectory* of $\vec{H}$ on $[0,T]$. The *Jacobi (or variational) equation* is the linear Hamiltonian dynamics: $\dot{\delta z}(t) = \frac{\partial \vec{H}}{\partial z}(z(t))\delta z(t)$ and a *Jacobi field* $J(t)$ is a (non zero) solution of this equation.

Definition 2.8. Consider a parameterized control system $\dot{x} = F(x,\lambda,u)$, $\lambda \in \Lambda \subset \mathbb{R}^q$ being the parameters set and denotes in short using the same notation $\dot{x} = F(x,u)$ by adding the dynamics $\dot{\lambda} = 0$, λ being considered as a fixed state component. Let $\vec{H}(z,u)$ be the Hamiltonian lift and let (z,u) be a (smooth) reference control trajectory on $[0,T]$. Fix an index i in the state space and denotes $(e_i)_i$ the canonical basis of vectors of the state space and let π_j be the standard projection $\pi_j : x \mapsto x_j$. The *sensitivity of the x_j-response to the x_i variable* (or parameter) is defined as

$$\mathcal{S}^{i,j}_{[0,T]} = \max_{t\in[0,T]} |\pi_j(J_i(t))|,$$

where $J_i(\cdot)$ is the Jacobi field with $J_i(0) = e_i$.

The following is useful for mathematical computations.

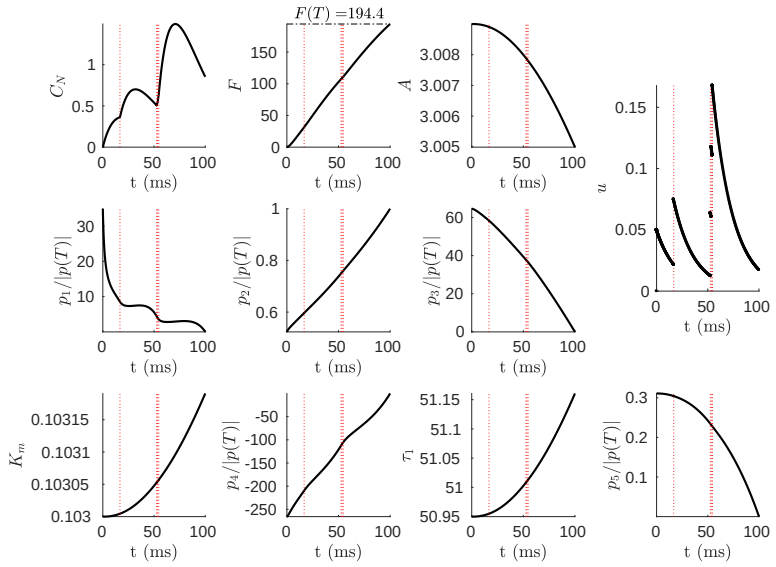

FIGURE 1. Extremal of the Ding et al. model defined on $[0,T]$, $T = 100ms$, with four sampling times and maximizing the final force.

Definition 2.9. Let H be a (smooth) Hamiltonian and denotes by $e^{t\vec{H}}$ the corresponding *one-parameter group* associated to $\vec{H}$. Write $\mathrm{ad}H(G) = \{H, G\}$, where G is a (smooth) mapping.

One has the following [1].

Proposition 3. *The Jacobi field is given by the (Hamiltonian) ad-formula*

$$J_i(t) = e^{tadH}(H_i)(z(t)) = \sum_{n\geq 0} \frac{t^n}{n!} ad^n H(H_i)(z(t)), \quad i = 1, \ldots, n,$$

where H_i stands for the Hamiltonian $p \cdot e_i$ and the right-hand side is converging for small t in the $\mathcal{C}^\omega$ (real analytic) case.

2.7 Sensitivity analysis

We consider the Ding et al. model and we present computations to analyze the sensitivity of the force variable F with respect to the fatigue variables A, K_m, τ_1 presented in Section 2.6. Take the reference extremal represented in Fig.1 satisfying the dynamics of the Ding et al. model defined on $[0,T]$, $T = 100$ms, such that $C_N(0) = F(0) = 0$, $A(0) = A_{rest} = 3.009$, $K_m(0) = K_{m,rest} = 0.103$, $\tau_1(0) = \tau_{1,rest}$, $p(T) = (0,1,0,0,0)$. We use the Hampath software to compute Jacobi fields, solutions of the variational equation (see Definition 2.7), obtained via automatic differentiation and numerical integration. More precisely,

- Fig.2 represents the time evolution of the Jacobi fields component $\delta F(\cdot)$, where the initialization corresponds to the canonical basis.
- Fig.3 represents the time evolution of the Jacobi fields component $\delta F(\cdot)$, where the initialization takes into account the physical values of the parameters $A_{\text{rest}}, K_{m,\text{rest}}, \tau_{1,\text{rest}}$.

It shows that the most sensitive variable is A and allows us to define a reduced model, where the fatigue parameters K_m and τ_1 are fixed to some constants.

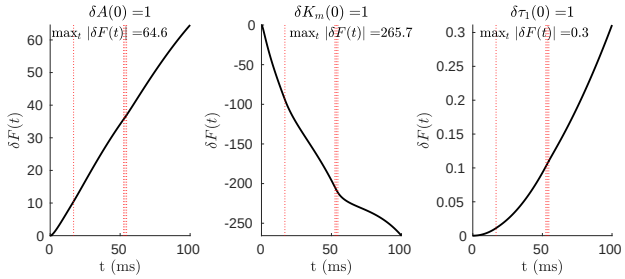

FIGURE 2. **Sensitivity analysis.** Time evolution of the Jacobi fields component $\delta F(\cdot)$ according to Definition 2.7 and associated to the trajectory of the force-fatigue model.

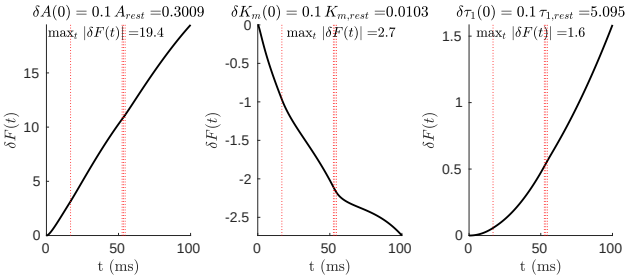

FIGURE 3. **Sensitivity analysis.** Time evolution of the Jacobi fields component $\delta F(\cdot)$ where their initializations are 10% of the physical values $A_{\text{rest}}, K_{m,\text{rest}}, \tau_{1,\text{rest}}$ associated to the trajectory of the force-fatigue model.

3 The geometric frame to analyze the control properties of the Marion et al. dynamics

3.1 The geometric frame

We refer to [8] for the concepts and results.

Definition 3.1. We consider the $\mathcal{C}^\omega$ single-input affine control system $\dot{x} = F_0(x) + u\, F_1(x)$ identified to the *polysystem* $D = \{F_0, F_1\}$, with $x \in \mathbb{R}^n$. The set of *admissible controls* is the set $\mathcal{U}$ of *bounded measurable* mappings $u : [0, T] \to U \subset \mathbb{R}$, with U being the control domain and $\mathcal{U}_c$ is the subset of piecewise constant mappings. The set $\mathcal{U}$ is endowed with the L^∞-norm topology: $\|u\| = \sup_{t\in[0,T]} |u(t)|$. If u is an admissible control on $[0, T]$, we denote $x(\cdot, x_0, u)$ the associated response, with $x(0) = x_0$, defined on a subinterval of $[0, T]$. Fix x_0 and T, the *extremity mapping* is the map $E^{x_0,T} : u \in L^\infty[0, T] \mapsto x(T, x_0, u)$. The *accessibility set in time* T is $A(x_0, T) = \cup_{u(\cdot)} x(T, x_0, u)$ and $A(x_0) = \cup_{T\geq 0} A(x_0, T)$ is the *accessibility set*.

Let X, Y be two $\mathcal{C}^\omega$-vector fields of $\mathbb{R}^n$ (identified to mappings valued in $\mathbb{R}^n$) and let $f : \mathbb{R}^n \to \mathbb{R}$ be a $\mathcal{C}^\omega$-mapping, we denote by Xf the *Lie derivative* (derivative of f in the X direction) and the *Lie bracket* is defined as $[X, Y] = Y \circ X - X \circ Y$ and is given in coordinates by $[X, Y](x) = X_x(x)Y(x) - Y_x(x)X(x)$. This defines the $\mathrm{ad}X$ *operator* by $\mathrm{ad}X(Y) = [X, Y]$. The Hamiltonian lift of X is $H_X(z) = p \cdot X(x)$, $z = (x, p)$ and Lie brackets and Poisson brackets are related by the formula $\{H_X, H_Y\}(z) = \mathrm{d}H_X(\vec{H}_Y)(z) = H_{[X,Y]}(z)$.

Consider the polysystem $D = \{F_0, F_1\}$, the *Lie algebra generated* by D, is denoted $D_{L.A.}$ and is defined recursively by $D_{L.A.} = \cup_{k\geq 1} D_k$ with $D_1 = \mathrm{span} D$, $D_k = \mathrm{span}\{D_{k-1} + [D, D_{k-1}]\}$ and to this flag we associate the following sequences of integers $n_k(x) = \dim D_k(x)$. For a pair of vector fields $\{F_0, F_1\}$ we can consider a *Hall basis* [10] and a *frame* at x_0 associated to D is a set of k-vectors fields of the Hall basis, such that at x_0 the dimension of the frame is equal to $D_{L.A.}(x_0)$.

Definition 3.2. We consider the polysystem $D = \{F_0 + u\, F_1,\ u \text{ (constant) } \in U\}$. This polysystem is associated to *controllability properties* with *piecewise constant* controls as follows (restricting the control set to $\mathcal{U}_c$). Take $x \in D$, we denote by e^{tX} the *one parameter group* associated to X and we denote by $S_T(D) = \left\{ e^{t_1 X_1} \circ \cdots \circ e^{t_k X_k},\ t_i \geq 0, k \geq 0, \sum_{i=1}^k t_i = T,\ X_i \in D \right\}$ and let $S(D)$ be the semi-group $\cup_{T\geq 0} S_T(D)$. Extending to $t_i \in \mathbb{R}$, we denote by $G(D)$ the group generated by $S(D)$.

The following properties are well known ([31]).

Properties 1. *One has*

1. $A(x_0, T) = S_T(D)(x_0)$
2. $A(x_0) = S(D)(x_0)$

One needs the following notations and results, see [22, 10].

Proposition 4. *In the C^ω category, take two vector fields X, Y and let φ be a local diffeomorphism. We have*

1. *Denote by $Z = \varphi * X$ the image of X by φ, then*
$$e^{tZ} = \varphi \circ e^{tX} \circ \varphi^{-1},$$
2. *The Baker-Campbell-Hausdorff formula is*
$$e^{sX} e^{tY} = e^{\zeta(X,Y)}, \quad \zeta(X, Y) \in \{X, Y\}_{L.A.}$$
and given for small s, t by the converging series
$$\zeta(X, Y) = sX + tY + \frac{st}{2}[X, Y] + \dots$$
3. *We have*
$$e^{tX} e^{Y} e^{-tX} = e^{t\mathrm{ad}X(Y)}$$
4. *The ad-formula is*
$$e^{tX} * Y = \sum_{k\geq 0} \frac{t^k}{k!} \mathrm{ad}^k X(Y)$$
and the series is converging for small t.

3.2 Singular trajectories

Again from [8], properties of nonlinear control systems in relation with optimal control are coded by singular trajectories that we introduce next. For convenience, we consider a general C^ω-control system $\dot{x} = F(x,u)$, $x \in \mathbb{R}^n$, $L^\infty \ni u : [0,T] \to U \subset \mathbb{R}^m$. As before, the extremity mapping for x_0, T, and denoted shortly E, is the mapping $L^\infty \ni u \mapsto x(T, x_0, u)$ extended to the control domain $U = \mathbb{R}^m$.

Proposition 5. *Let $x(\cdot), u(\cdot)$ be a control trajectory reference defined on $[0,T]$ and let $\delta v(\cdot)$ be a L^∞-perturbation.*

1. *The extremity mapping is Fréchet differentiable at u, the Fréchet derivative coincides with the Gâteaux derivative and is solution of the variational equation*
$$\dot{\delta_1 x}(t) = A(t)\delta_1 x(t) + B(t)\delta v(t) \qquad a.e. \tag{18}$$
with $\delta_1 x(0) = 0$, $A(t) = f_x(x(t), u(t))$, $B(t) = f_u(x(t), u(t))$.
2. *If M denotes the fundamental matrix solution of $\dot{M} = AM$, with $M(0)$ being the identity matrix, and if $\Phi(t,s)$ is the state transition matrix: $\Phi(t,s) = M(t)M^{-1}(s)$, one has*
$$E'_u(\delta v) = \int_0^T \Phi(T,t)B(t)\delta v(t)\,\mathrm{d}t.$$

Definition 3.3. *A singular control trajectory pair $(x(\cdot), u(\cdot))$* on $[0,T]$ is a singularity of the Fréchet derivative at u, that is the dimension of $\mathrm{Im}E'$ is strictly smaller than the dimension of the state space.

The key point for computations is the *method of saturation* in algebraic geometry, which leads to the so-called weak Pontryagin Maximum Principle, introducing the Hamiltonian formalism.

Proposition 6. *Consider the Hamiltonian lift of the system $H(z,u) = p \cdot F(x,u)$ called the pseudo-Hamiltonian in control theory. If the pair $(x(\cdot), u(\cdot))$ is singular on $[0,T]$ then there exists a triple (z,u), $z = (x,p)$, $p \neq 0$ called an extremal on $[0,T]$ such that the following holds*

1. $$\dot{x} = \frac{\partial H}{\partial p}, \quad \dot{p} = -\frac{\partial H}{\partial x} \qquad a.e. \tag{19}$$
2. $$\int_0^T p(t)B(t)\delta v(t)\,\mathrm{d}t = 0 \tag{20}$$
for every $\delta v(\cdot) \in L^\infty$.
3. *The second condition can be written as*
$$\frac{\partial H}{\partial u} = 0 \qquad a.e. \tag{21}$$

Note that the formulation with (20) is crucial in the frame of optimal sampled-data control.

Algorithm to compute singular controls. One uses the proposition 6, especially the relation $\frac{\partial H}{\partial u} = 0$, which leads to consider the regular and totally singular case, in the case of affine systems.

Case 1: Assume the condition $\frac{\partial^2 H}{\partial u^2} \neq 0$ on $[0,T]$ and solve $\frac{\partial H}{\partial u} = 0$ using the implicit function theorem. Then the singular control can be written locally as a $\mathcal{C}^\omega$-function denoted $\hat{u}(z)$. Plugging $\hat{u}$ in H defines the true Hamiltonian $\hat{H}(z) = H(z, \hat{u})$. Then the pair $z = (x, p)$ is solution of $\dot{z} = \vec{\hat{H}}(z)$.

Case 2: Assume $F(x,u) = F_0(x) + u\, F_1(x)$. Then $\frac{\partial H}{\partial u} = 0$ amounts to $H_1(z) = p \cdot F_1(x) = 0$. Differentiating twice with respect to time, one gets the relations:

$$\begin{aligned} &H_1(z) = \{H_1, H_0\}(z) = 0 \\ &\{\{H_1, H_0\}, H_0\}(z) + u\, \{\{H_1, H_0\}, H_1\}(z) = 0 \end{aligned} \tag{22}$$

with $H_0(z) = p \cdot F_0(x)$.

One introduces the following.

Definition 3.4. A singular extremal (z,u) is called of *minimal order* on $[0,T]$ if $\{\{H_1, H_0\}, H_1\}(z(t)) \neq 0$ for every t and of *higher order* if one has $\{\{H_1, H_0\}, H_1\}(z(t)) = 0$ for every t.

Corollary 1. *Let $\hat{H}(z) = H(z, \hat{u})$, where $\hat{u}$ is solution of (22) be the (true) Hamiltonian. Then minimal order extremals are solutions of the associated constrained Hamiltonian equation $\dot{z} = \vec{\hat{H}}(z)$ with $H_1(z) = \{H_1, H_0\}(z) = 0$.*

3.3 Application to the Marion et al. model

We proceed to simplify algebraic computations in two steps, which capture the crucial geometric properties.

3.3.1 Fatigue model

Consider first the fatigue variables dynamics (17) written as the linear system $\dot{\bar{x}} = \lambda_2 I_3\, \bar{x} + u_1 \alpha + u_2 \beta$ with $\bar{x} = (A_{90} - A_{90,rest}, K_m - K_{m,rest}, \tau_1 - \tau_{1,rest})^\intercal$ and $u_1 = F$, $u_2 = \dot{\theta}\, F$, taken as control variables. Let $D = \{\lambda_2 I_3 x, \alpha, \beta\}$ be the associated polysystem ($u_1, u_2 \in \mathbb{R}$).

Lemma 3.5. *At $\bar{x} = 0$, the Lie algebra $D_{L.A.}$ is* $\operatorname{span}\{\alpha, \beta\}$.

Proof. This is clear since the free dynamics is described by the identity matrix. □

Geometric application From our previous analysis, we can restrict our system to the most sensitive fatigue variables, using sensitivity concept defined in section 2.6.

3.3.2 Construction of a frame and singular trajectories in the Marion et al. model

To simplify the computations, one can consider only the model where the fatigue variables are taken as fixed parameters, and the system is written as (F_0, F_1), the state space being $x = (x_1, x_2, x_3, x_4)^\intercal$ and from section 2.3, one has

$$F_0(x) = (\lambda_1 x_1, \sigma(x_3, x_4) m_1(x_1) - x_2 m_2(x_1), x_4, \ell_1 \cos x_3 - \ell_2 x_2)^\intercal$$

and $F_1 = (1,0,0,0)^\intercal$. To compute iterated Lie (Poisson) brackets, one uses the following notations:

$$F_{10} = \mathrm{ad}F_1(F_0), \quad H_{10} = \mathrm{ad}H_1(H_0),$$

and recursively,

$$F_{ij} = \mathrm{ad}F_i(F_j), \quad H_{ij} = \mathrm{ad}H_i(H_j),$$

where i is a sequence of integers valued in $\{0,1\}$ and $j \in \{0,1\}$.

Now, in relation with singular extremals computations, we introduce the following *Goh transformation*, in our context, see [8].

Definition 3.6. Note that $m_1 : x_1 \mapsto m_1(x_1)$ is an increasing mapping from $[0,+\infty)$ to the interval $[0,1]$ and take $m_1 = v$ as the *accessory control*, while $m_2(v) = 1/(\tau_1 + \tau_2 v)$. The *reduced system* associated to the following *Goh transformation* is the control system on the $x = (x_2, x_3, x_4)^\intercal$-space defined by $F(x,v) = (\sigma(x_3,x_4)v - x_2 m_2(v), x_4, \ell_1 \cos x_3 - \ell_2 x_2)^\intercal$.

Next, we proceed to the computations of Lie brackets in relation with the *stratification* associated to singular extremals computations [7].

First, one has: $F_{01}(x) = [F_0, F_1](x) = \frac{\partial F_0}{\partial x_1}(x) = (\lambda_1, \sigma(x_3,x_4)m_1' - x_2 m_2', 0, 0)^\intercal$ and note that F_{01} is colinear to F_1 on the set

$$S_1 : \sigma(x_3,x_4)m_1'(x_1) - x_2 m_2'(x_1) = 0, \tag{23}$$

and outside S_1 one has

$$\mathrm{span}\{F_1, F_{01}\} = \mathrm{span}\left\{\frac{\partial}{\partial x_1}, \frac{\partial}{\partial x_2}\right\}.$$

Since $v = m_1$, $m_2(v) = \frac{1}{\tau_1 + \tau_2 v}$, the equation (23) of S_1 is equivalent to

$$S_1 : \sigma(x_3,x_4)(\tau_1 + \tau_2 v)^2 + x_2\tau_2 = 0, \tag{24}$$

and since σ can takes positive and negative values, one gets solution of the form

$$\tau_1 + \tau_2 v = \sqrt{-\frac{x_2\tau_2}{\sigma}}, \quad \text{when } \sigma < 0. \tag{25}$$

Moreover one has, $[[F_0,F_1],F_1](x) = (0, \sigma m_1'' - x_2 m_2'', 0, 0)^\intercal$.
From the above computations, we deduce the following.

Proposition 7. *The relations $H_1 = H_{10} = H_{100} + u\, H_{101} = 0$ lead to*

1. *Admissible singular trajectories in*
$$S_1 : \sigma m_1'(x_1) - x_2 m_2'(x_1) = 0$$
with admissible control defined by (25).
2. *Outside of S_1, one has $p_1 = p_2 = 0$ and $H_{101} = 0$. Hence there exists no minimal order singular extremals.*

Further computations give

$$F_{100} = (-\sigma m_1' + x_2 m_2')\ell_2 \frac{\partial}{\partial x_4} \mod \left\{\frac{\partial}{\partial x_1}, \frac{\partial}{\partial x_2}\right\}$$

and denoting $G = (-\sigma m_1' + x_2 m_2')\frac{\partial}{\partial x_4}$, one has

$$\begin{aligned} [G, F_1] &= (-\sigma m_1'' + x_2 m_2'')\frac{\partial}{\partial x_4}, \\ [G, F_0] &= (-\sigma_{x_3} m_1' x_4)\frac{\partial}{\partial x_3}, \quad \mod \left\{\frac{\partial}{\partial x_1}, \frac{\partial}{\partial x_2}, \frac{\partial}{\partial x_4}\right\} \end{aligned} \tag{26}$$

Hence, outside S_1, the relation

$$H_1 = H_{10} = H_{101} = H_{100} = 0$$

leads to $p_1 = p_2$ and $p_4 = 0$.
Moreover $H_{1000} + u\, H_{1001} = 0$ leads to the relation

$$S_2 : x_4 \sigma_{x_3}(x_3, x_4) = 0 \tag{27}$$

in the physical space $(\theta, \dot{\theta})$.

In particular, this gives a frame construction for geometric computations using Baker-Campbell-Hausdorff formula outside $S_1 \cup S_2$: $F_0, F_1, F_{01}, F_{100}$ and note moreover that $F_1, F_{01}, F_{100}, F_{1000}$ are linearly independent.

Moreover this concludes the discussion about higher-order singular arcs using relation (27).

4 Pontryagin necessary optimality conditions in the permanent or standard case vs the sampled-data control case

The *calculus of variations* finds its origin in the Jacobi brachistochrone problem at the end of the 17th century, see the seminal references [20, 6] for a neat presentation. It concerns optimality conditions, for *piecewise smooth* curves, and they are derived using specific curves variations and an abundance of conditions. *Optimal control* and the Pontryagin Maximum Principle [26] was a revival of the whole area and a true revolution. Indeed, it allows to consider absolutely continuous curves and to take into account control bounds, to provide a direct Hamiltonian formulation. Moreover, see the historical presentation [19], the necessary optimality conditions were obtained using only one set of L^1-control variations called needle or Weierstrass variations. Later, in the frame of geometric conditions, the necessary optimality conditions were interpreted in the context of symplectic geometry and generalized to second-order conditions, see for instance [1]. These contributions led to mathematical analysis of practical optimal control problems, for instance in biology [30].

The sampled-data case motivated by digital controls is an intermediate case between calculus of variations and the general frame of Pontryagin Maximum Principle. Indeed, in [11], the authors consider L^∞ variations over a fixed interval, while time variations are considered in [12]. Due to the structure of the FES-input and the phenomenon of tetania, *specific necessary Pontryagin type* conditions have to be derived to deal with our muscular control problem, see [4] for the detailed presentation. The aim of this section is to make a discussion of the necessary conditions in the permanent case vs the sampled-data case to analyze the non-isometric Marion et al. model.

4.1 Maximum Principle in the permanent case

One considers a general (smooth) control system of the form

$$\dot{x}(t) = f(t, x(t), u(t)), \quad x(t) \in \mathbb{R}^n \tag{28}$$

and in the *permanent* (standard) case, the set of admissible controls is the set $\mathcal{U}$ of all bounded measurable mappings $u(\cdot)$ on $[0, T]$ valued in $U \in \mathbb{R}^m$ (control domain). For the application and simplicity of the presentation we shall consider only the Mayer optimal control problem $\min_{u(\cdot)} \varphi(x(T))$ where φ is a (smooth) function.

We denote as usual by H the Hamiltonian lift defined by $H(t, z, u) = p \cdot f(t, x, u)$, $z = (x, p)$.

Recall that the Pontryagin necessary optimality conditions are obtained as follows. Let x^* be a reference optimal curve on $[0,T]$, associated to $u^* \in \mathcal{U}$. A *needle variation* of the reference control is defined by $u_\varepsilon(t) = v \in U$ fixed on $[s, s+\varepsilon]$, where s is a *Lebesgue time* of the reference trajectory, $\varepsilon > 0$ and $u_\varepsilon(t) = u^*(t)$ elsewhere. Denote by $x^*_\varepsilon(\cdot)$ the corresponding trajectory. This control variation leads to the *variation vector* defined as

$$w(s) = \lim_{\varepsilon \to 0^+} \frac{x^*_\varepsilon(s) - x^*(s)}{\varepsilon} \tag{29}$$

and a simple computation, since s is a Lebesgue time, gives

$$w(s) = f(s, x^*(s), v) - f(s, x^*(s), u^*(s)). \tag{30}$$

Introduce the corresponding variation vector solution of the linear dynamics

$$\dot{w}(t) = f_x(t, x^*(t), u^*(t))w(t) \tag{31}$$

with the initial condition $w(s)$ given by (30). From optimality one gets

$$\frac{\varphi(x^*_\varepsilon(T)) - \varphi(x^*(T))}{\varepsilon} \geq 0$$

and taking the limit as $\varepsilon \to 0^+$, one obtains the condition

$$\varphi_x(x^*(T)) \cdot w(T) \geq 0. \tag{32}$$

Introduce the adjoint equation

$$\dot{p}(t)^\intercal = -p(t)^\intercal f_x(t, x^*(t), u^*(t)) \tag{33}$$

with $p(T) = -\varphi_x(x^*(T))$.

Denote by $\Phi(\cdot,\cdot)$ the state-transition matrix associated to (31). Using inequality (32) and the relations

$$w(T) = \Phi(T,s)w(s), \quad p(s) = \Phi(T,s)^\intercal p(T)$$

and since $p(t) \cdot w(t)$ is constant, one deduces the inequality

$$p(s) \cdot (f(s, x^*(s), v) - f(s, x^*(s), u^*(s))) \leq 0. \tag{34}$$

This leads to the Pontryagin Maximum Principle in the permanent case.

Proposition 8. *In the permanent case one has the maximization condition*

$$H(s, x^*(s), p(s), u^*(s)) = \max_{v \in U} H(s, x^*(s), p(s), v) \quad \text{a.e. on } [0,T]. \tag{35}$$

4.2 The sampled-data control case

Consider the previous problem and the case where the set of controls on $[0,T]$ is restricted to the set of constant controls on a *fixed subdivision* $t_0 = 0 < t_1 < \cdots < t_n < T = t_{n+1}$, that is $u = u_i$ constant on $[t_i, t_{i+1}]$, $i = 0, \ldots, n$.

Take a reference optimal control u^* in this category defined by u^*_i constant on $[t_i, t_{i+1}]$. The control domain being convexified, consider the L^∞-perturbation of the reference control defined by $u_\varepsilon = u^* + \varepsilon(u - u^*)$, with $u = u_i$ on $[t_i, t_{i+1}]$.

Using section 3.2, the corresponding variation vector $w(t)$ satisfies the equation

$$\dot{w}(t) = A(t)w(t) + B(t)(u(t) - u^*(t)) \tag{36}$$

with $w(0) = 0$ and $A(t) = f_x(t, x^*(t), u^*(t))$, $B(t) = f_u(t, x^*(t), u^*(t))$. Integrating one gets

$$w(T) = \int_0^T \Phi(T, s)B(s)(u(s) - u^*(s))\,\mathrm{d}s \leq 0.$$

Using as before the inequality (32), one gets the condition

$$\int_0^T p(s)B(s)(u(s) - u^*(s))\mathrm{d}s \leq 0. \tag{37}$$

Since the controls are constant on each fixed interval $[t_i, t_{i+1}]$, one gets the proposition.

Proposition 9. *In the sampled-data case, with fixed interpulses one gets the necessary optimality condition*

$$\left(\int_{t_i}^{t_{i+1}} p(s)B(s)\mathrm{d}s\right) \delta u_i \leq 0 \tag{38}$$

for each admissible variation δu_i.

One can proceeds similarly to derive necessary conditions with free sampling times. This approach is used next to derive the conditions for our muscular control problem.

4.3 Pontryagin type necessary conditions in the muscular problem

They were determined in [3] for the isometric case but are similar in the non-isometric case. They are given next and we sketch the proof, in relation with the concepts introduced in this article. The system is written as

$$\begin{aligned} \dot{x}(t) &= g(x(t)) + b(t)\left(\sum_{i=0}^{n} G(t_{i-1}, t_i)\eta_i H(t - t_i)\right) e_1 \\ x(0) &= x_0, \end{aligned} \tag{39}$$

where $b(t) = \frac{1}{\tau_c}e^{-t/\tau_c}$, $G(t_{i-1}, t_i) = (R_0 - 1)e^{t_{i-1}/\tau_c} + e^{t_i/\tau_c}$, $t_{-1} = -\infty$, $t_0 = 0$, $t_{n+1} = T$ and $e_1 = (1, 0, \ldots, 0)^\intercal$.

The first step is to define the admissible perturbations.

4.3.1 Admissible perturbations

The set of controls is parameterized by $\delta = (\eta_0, \ldots, \eta_n, t_1, \ldots, t_n) \in \mathbb{R}^{2n+1}$ with the following constraints

- $\eta_i \in [0, 1],\ \forall i = 0, \ldots, n,$
- $0 < t_1 < \cdots < t_n < T,\ t_i - t_{i-1} \geq I_m,\ \forall i = 1, \ldots, n.$

Hence the set of $\mathcal{P}$ admissible perturbations is defined as follows.

Definition 4.1. The set of admissible perturbation $\bar{\delta} = (\bar{\eta}_0, \ldots, \bar{\eta}_n, \bar{t}_1, \ldots, \bar{t}_n) \in \mathcal{P}$ decomposes as follows

(i) For $i = 0, \ldots, n$, we say that $\bar{\eta}_i \in \mathbb{R}$ is an admissible perturbation of η_i if there exists $\bar{\varepsilon} > 0$ such that $\eta_i + \varepsilon\bar{\eta}_i \in [0, 1]$ for all $0 \leq \varepsilon \leq \bar{\varepsilon}$.

(ii) For $i = 1, \ldots, n-1$, we say that $\bar{t}_i \in \mathbb{R}$ is an admissible perturbation of t_i if there exists $\bar{\varepsilon} > 0$ such that $(t_i + \varepsilon\bar{t}_i) - t_{i-1} \geq I_m$ and $t_{i+1} - (t_i + \varepsilon\bar{t}_i) \geq I_m$ for all $0 \leq \varepsilon \leq \bar{\varepsilon}$.

(iii) For $i = n$, we say that $\bar{t}_n \in \mathbb{R}$ is an admissible perturbation of t_n if there exists $\bar{\varepsilon} > 0$ such that $(t_n + \varepsilon \bar{t}_n) - t_{n-1} \geq I_m$ for all $0 \leq \varepsilon \leq \bar{\varepsilon}$.

4.3.2 Pontryagin type necessary optimality conditions

Proposition 10. *Let x^* be an optimal solution on $[0,T]$ with corresponding sampled-data optimal control $\delta^* = (\eta_0^*, \dots, \eta_n^*, t_1^*, \dots, t_n^*)$ and let $\delta = (\bar{\eta}_0, \dots, \bar{\eta}_n, \bar{t}_1, \dots, \bar{t}_n)$ be an admissible perturbation. Then there exists an adjoint vector $p^* = (p_1^*, \dots, p_n^*)^\intercal$ solution of*

$$\begin{aligned} \dot{p}(t)^\intercal &= -p(t)^\intercal g_x(x^*(t)) \quad \text{a.e. on } [0,T] \\ p(T) &= -\varphi_x(x^*(T)), \end{aligned}$$

such that

(i) *the inequality*

$$\left(\int_{t_i^*}^{T} p_1(s) b(s) \, \mathrm{d}s \right) \bar{\eta}_i \leq 0, \tag{40}$$

for all $i = 0, \dots, n$ and all admissible perturbation $\bar{\eta}_i$ of η_i^*;

(ii) *and the inequalities*

$$\begin{aligned} \Bigg(- p_1(t_i^*) b(t_i^*) G(t_{i-1}^*, t_i^*) \eta_i^* + b(-t_i^*) \eta_i^* \int_{t_i^*}^{T} p_1(s) b(s) \, \mathrm{d}s \\ + b(-t_i^*)(R_0 - 1) \eta_{i+1}^* \int_{t_{i+1}^*}^{T} p_1(s) b(s) \, \mathrm{d}s \Bigg) \bar{t}_i \leq 0, \end{aligned} \tag{41}$$

for all $i = 1, \dots, n$ and all admissible perturbation $\bar{t}_i$ of t_i^*,

are satisfied.

Proof. First of all, note that (i) follows directly form (37). Let us prove the second case (ii). The computation is straightforward since the control enters directly only in the x_1 coordinate equation corresponding to the evolution of the Ca^{2+}-concentration and moreover this dynamics is linear and can be integrated, see (5). In particular, take a t_i-variation and let write the variations as $w(t) = (w_1(t), w_2(t)) \in \mathbb{R} \times \mathbb{R}^{n-1}$ and using (36) a direct computation gives that w_1 is solution of the equation

$$\begin{aligned} \dot{w}_1(t) &= -\frac{w_1(t)}{\tau_c} + \bar{t}_i b(t) b(-t_i^*) \eta_i^* + (R_0 - 1) \eta_{i+1}^* H(t - t_{i+1}^*) \text{ a.e. on } [t_i, T] \\ w_1(t_i^*) &= -\bar{t}_i (b(t_i^*) G(t_{i-1}^*, t_i^*) \eta_i^*). \end{aligned} \tag{42}$$

Integrating w_1, this corresponds precisely to compute the derivative of x_1 with respect to t_i in the direction $\bar{t}_i$ over $[t_i, T]$ (Gâteaux derivative) and we deduce the inequality (ii). □

Definition 4.2. Let $\delta^* = (\eta_0^*, \dots, \eta_n^*, t_1^*, \dots, t_n^*)$ be an optimal control. It is called η_i-saturating if $\eta_i^* = 0$ or 1 and t_i-saturating if $t_i^* - t_{i-1}^* = I_m$ and non saturating otherwise.

Corollary 2. *In the non saturating case the corresponding inequalities in proposition 10 lead to equality.*

4.4 The sampled-data case vs the permanent case in the Marion et al. model

In the muscular control problem, the formulation using the FES-input gives precisely the sampled-data control frame and the necessary optimality condition of proposition 10. In this form, they have to be numerically handled to provide the structure of the optimal solution, which decomposes into arcs saturating the amplitude η_i^* over $[t_i^*, t_{i+1}^*]$ or the minimal interpulse that $t_i^* - t_{i-1}^* = I_m$. Only in a few obvious cases, one can have information about this saturation. One important case being when, in the short stimulation protocol, one must maximize the force and hence clearly the optimal control is η_i-saturating for all $i = 0, \dots, n$. Over a long period, the stimulation protocol has to take into account the minimization of the fatigue, which mathematically leads to explore the adjoint system with an adjoint vector $p^*(T)$ not colinear to $(0, 1, 0, \dots, 0)^\intercal$. On the opposite, the Maximum Principle in the permanent case can give mathematical information about the structure of the optimal solution, which splits into regular and singular arcs, regular arcs corresponding to saturating controls. Moreover the switches can be evaluated. In the geometric frame of section 3, this leads to analyze in particular the accessory problem introduced in definition 3.6 and concerning the problem where the accessory control is given by the Ca^{2+}-concentration.

5 Numerical algorithms and numerical simulations

We have addressed two optimization problems (OC1)-(OC2) in Section 2.5 related to the Ding et al. model and Marion et al. model and we present in this section a direct approach and an indirect approach to solve them. We first present the algorithms of the two methods and give the numerical results for the two models.

We fix the amplitudes η_i, $i = 1, \dots, n$ and we consider the finite dimensional optimal control problem

$$\begin{cases} \min\limits_{\delta} \ \varphi(x(T)) \\ \dot{x}(t) = f(x(t), \delta) \ a.e. \ t \in [0, T], \\ x(0) = x_0, \end{cases} \tag{43}$$

where $\delta = (t_i)_{i=1,\dots,n}$, T being fixed, $\varphi(x(T)) = w_1 F(T) + w_2 D(T)$ (D being a fatigue variable) and the dynamics f is defined from the Ding et al. model or the Marion et al. model.

5.1 Algorithms

5.1.1 Direct method

Given a subdivision of $[0, T]$, we discretize the problem (43) to obtain a nonlinear finite dimensional optimization problem, where the optimization variables are $t_1, \dots, t_n$, the cost is $\varphi(x(T))$ and the constraints are defined by the discretized dynamics. We implement a primal-dual interior point method from the `IPOPT C++` library to solve this optimization problem. The derivatives of the objective and constraints being computed via automatic differentiation (package `CppAD`). This algorithm was implemented successfully for the Ding et al. model in [4] and in this article we use this method as a benchmark (see [3, 4] for further details).

5.1.2 Indirect method

Augmented dynamics. For $i = 1, \dots, n$, we introduce the new variables y_i such that $\dot{y}_i(t) = H(t - t_i)\, p_1(t) b(t)$ and $y_i(0) = 0$ (H being the Heaviside function) and we have $y_i(T) = \int_{t_i}^{T} p_1(t) b(t) \mathrm{d}t$.
Discretization. We discretize the dynamics with respect to a subdivision $\mathcal{T} = (s_1, \dots, s_N)$ of $[0, T]$ and the discretized state-adjoint vectors are denoted by $X^{\mathcal{T}} := (x(s_1), \dots, x(s_N))$, $P^{\mathcal{T}} := (p(s_1), \dots, p(s_N))$ and $Y_i^{\mathcal{T}} := (y_i(s_1), \dots, y_i(s_N))$, $i = 1, \dots, n$.

The aim is to compute $\delta = (t_1, \dots, t_n)$, $p(0) = p(s_1)$ such that

$$
\begin{aligned}
&x(s_{j+1}) = K_x(\mathcal{T}, X^{\mathcal{T}}, P^{\mathcal{T}}, \delta),\\
&p(s_{j+1}) = K_p(\mathcal{T}, X^{\mathcal{T}}, P^{\mathcal{T}}, \delta),\\
&y_i(s_{j+1}) = K_{y_i}(\mathcal{T}, P^{\mathcal{T}}, Y_i^{\mathcal{T}}, \delta),\\
&x(s_1) = x_0,\ p(s_1) = p_0,\ y_i(s_1) = 0,\ p(s_N) = -\nabla\varphi(x(s_N)) = (0, 1, 0, 0, 0)^\intercal \qquad (44)\\
&I_m + t_j - t_{j+1} \le 0, \quad j = 0, \dots, n\\
&\alpha_i = \operatorname{sign}(t_{i+1} - t_i - I_m) + 1, \quad \beta_i = \operatorname{sign}(t_i - t_{i-1} - I_m) + 1,\\
&f_i(P^{\mathcal{T}}, y_i(T), \delta)\, \alpha_i \le 0, \quad f_i(P^{\mathcal{T}}, y_i(T), \delta)\, \beta_i \ge 0,
\end{aligned}
$$

for all $1 \le j \le N - 1$, $1 \le i \le n$ and where x_0 is given, K_x, K_p and K_{y_i}, $i = 1, \dots, n$ stand for a discretization scheme of the dynamics of x, p and y_i, $i = 1, \dots, n$ respectively, and $f_i(P^{\mathcal{T}}, y_i(T), \delta) = -p_1(t_i) b(t_i) G(t_{i-1}, t_i) + b(-t_i) y_i(T) + b(-t_i)(R_0 - 1) y_{i+1}(T)$, $i = 1, \dots, n$ typify the inequalities (41).

Then, the boundary value problem (44) is formulated as a nonlinear finite dimensional optimization problem of the form

$$
\min_{\substack{\delta \in \mathbb{R}^n \\ p_0 \in \mathbb{R}^5}} \quad \Phi(X^{\mathcal{T}}, P^{\mathcal{T}}, Y_1^{\mathcal{T}}, \dots, Y_n^{\mathcal{T}}, \delta)
$$

where

$$
\begin{aligned}
\Phi(X^{\mathcal{T}}, &P^{\mathcal{T}}, Y_1^{\mathcal{T}}, \dots, Y_n^{\mathcal{T}}, \delta) =\\
&\sum_{i=1}^{n} \left(\log(-f_i(P^{\mathcal{T}}, y_i(T), \delta)\alpha_i) + \log(f_i(P^{\mathcal{T}}, y_i(T), \delta)\beta_i) \right),
\end{aligned}
$$

and subject to

$$
\begin{aligned}
&x(s_{j+1}) = K_x(\mathcal{T}, X^{\mathcal{T}}, P^{\mathcal{T}}, \delta),\\
&p(s_{j+1}) = K_p(\mathcal{T}, X^{\mathcal{T}}, P^{\mathcal{T}}, \delta),\\
&y_i(s_{j+1}) = K_{y_i}(\mathcal{T}, P^{\mathcal{T}}, Y_i^{\mathcal{T}}, \delta),\ j = 1, \dots, N - 1,\ i = 1, \dots, n,\\
&x(s_1) = x_0,\ p(s_1) = p_0,\ y_i(s_1) = 0,\ p(s_N) = -\nabla\varphi(x(s_N)) = (0, 1, 0, 0, 0)^\intercal\\
&I_m + t_i - t_{i+1} \le 0, \quad i = 0, \dots, n - 1.
\end{aligned}
$$

As in the direct method, we solve this optimization problem with a primal-dual interior point method and the derivatives of the objective and of the constraints are computing using automatic differentiation (package `CppAD`).

5.2 Preliminary numerical results

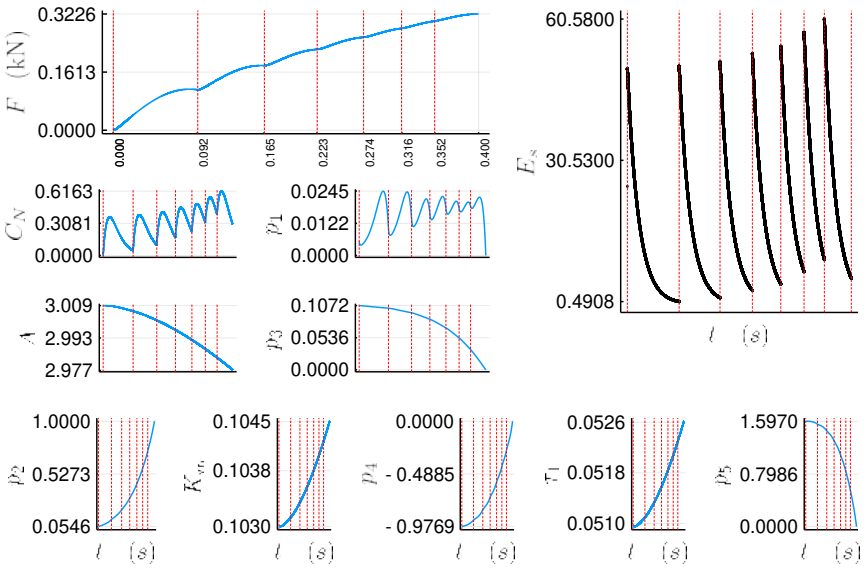

FIGURE 4. Time evolution on $[0,T]$, $T = 0.4s$ of the state of the Ding et al. model computed with the indirect approach maximizing $\varphi(x(T)) = F(T)$ with $n = 6$, $I_m = 20$ms. The optimal value is the same as the optimal value computed with the direct method (see Fig.5). The model parameters are given in Table 1.

We present the numerical results of the direct method for the Marion et al. model and show that the two methods yield the same optimal solutions for the Ding et al. model.

5.2.1 Ding et model

In Figs.4,5 we represent the solutions for the Ding et al. model the case $n = 6$ and $T = 0.4$s, where we maximize $\varphi(x(T)) = F(T)$, respectively with the indirect method and the direct method. The direct method is computationally more efficient than the indirect method, it converges in fewer iterations and it can handle larger number of sampling times over a larger time interval. We recover the same optimal value than the direct method with $F(T) = 322.6$N but attained for different optimal values of δ. Again, the constraints $t_{i+1} - t_i \geq I_m,\ i = 1, \ldots, n-1$ are not saturating.

5.2.2 Marion et al. model

Fig.6 gives the solution obtained with the direct method with $n = 10$, $T = 0.9$s, $x_0 = (0, 0, A_{90,0}, K_{m_0}, \tau_{1,0})$, $I_m = 20$ms and the values of the parameters of the model are given in Table 2. Note we have considered the normalized state variable $(C_N, F/F_{ext}, A_{90}/A_{90,0}, K_m/K_{m,0}, \tau_1/\tau_{1,0})$. We observe a rest period while maximizing $\varphi(x(T)) = F(T)/F_{ext} + A_{90}(T)/A_{90,0}$ and this solution has to be compared with the sub-optimal policy $t_i = T - (n-i+1)I_m$, $i = 1, \ldots, n$ given in Fig.7. Note that the optimal solution represented in Fig.6 is not saturating the constraints $t_{i+1} - t_i \geq I_m,\ i = 1, \ldots, n-1$.

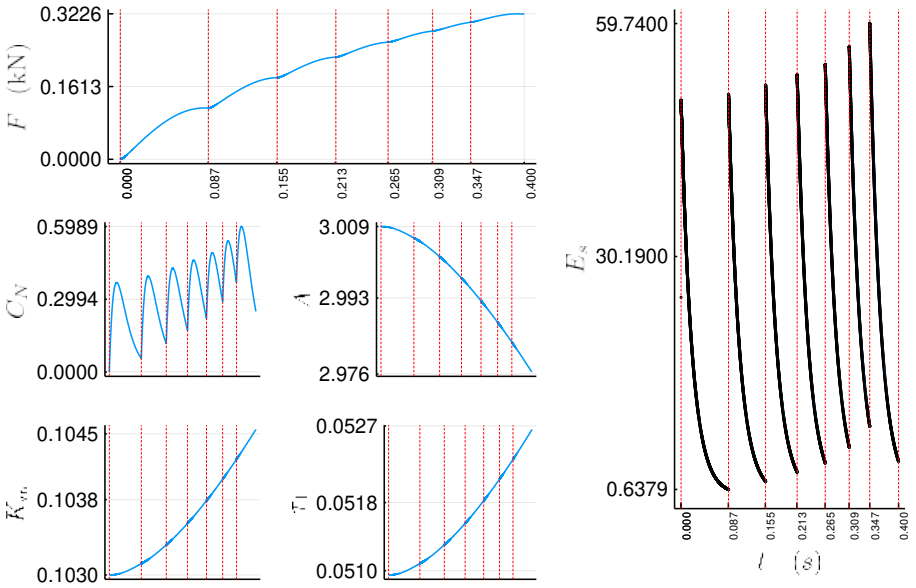

FIGURE 5. Time evolution on $[0, T]$, $T = 0.4s$ of the normalized state of the Ding et al. model computed with the direct approach maximizing $\varphi(x(T)) = F(T)$ with $n = 6$, $I_m = 20$ms. The model parameters are given in Table 1.

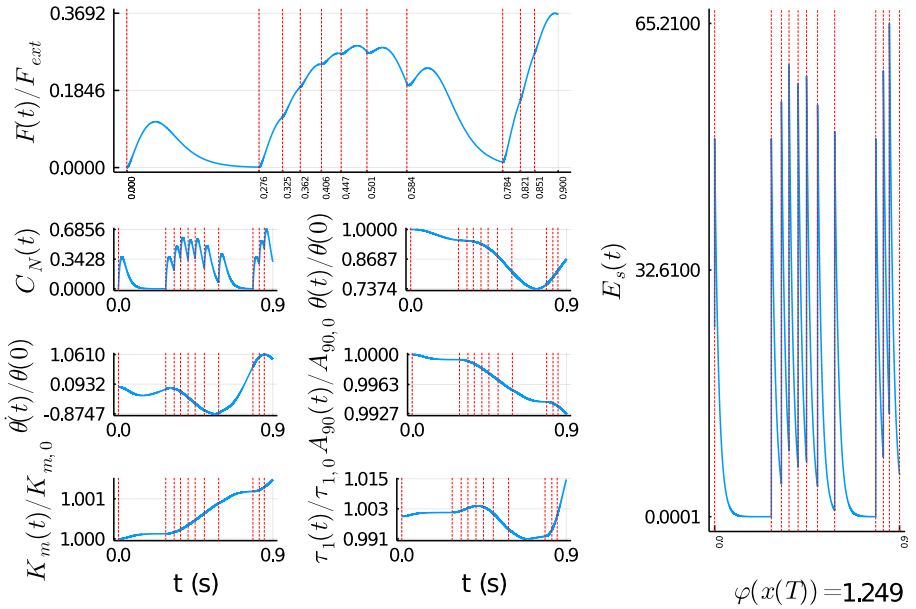

FIGURE 6. Time evolution on $[0, T]$, $T = 0.9s$ of the normalized state of the Marion et al. model computed with the direct approach maximizing $\varphi(x(T)) = F(T)/F_{ext} + A_{90}(T)/A_{90,0}$ with $n = 10$, $I_m = 20$ms. The model parameters are given in Table 2.

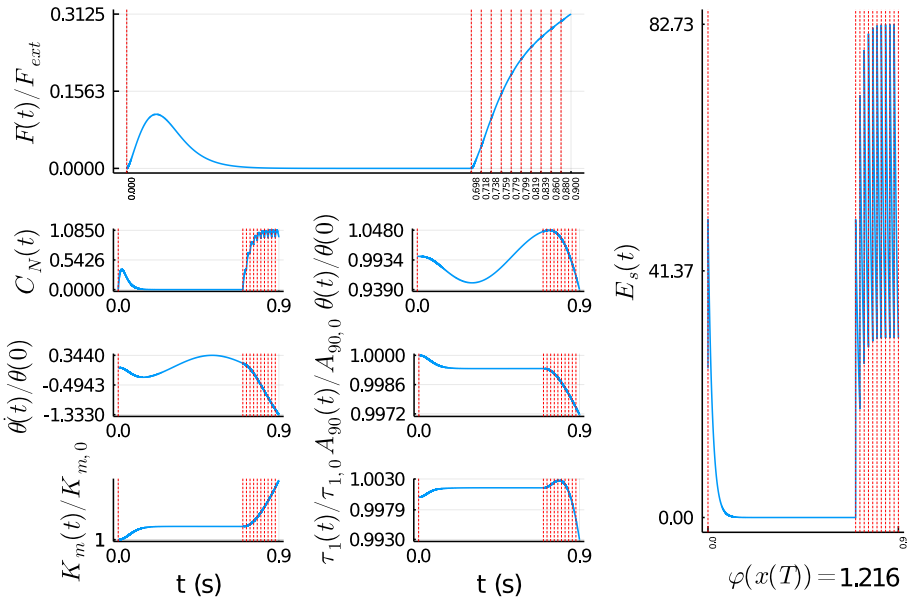

FIGURE 7. Time evolution on $[0, T]$, $T = 0.9s$ of the normalized state of the Marion et al. model with the direct method when considering $t_i = T-(n-i+1)I_m$, $i = 1, \ldots, n$, $n = 10$, $I_m = 20ms$. The model parameters are given in Table 2.

6 Conclusion

In this article, we have presented the geometric techniques to analyze the optimality problems in the muscular force-fatigue model, extending the isometric case to the non-isometric case and presenting preliminary numerical algorithms and results to validate our techniques. Additional work is required in the future in two directions. First, efficient algorithms have to be found adapted to the resolution of the Hamiltonian variational inequalities related to the problem, in the case of a sequence of several pulses trains, over a large final time T. Second, numerous simulations are necessary to understand the structure of the optimal solutions, corresponding to the experimental optimal problems.

We have restricted our analysis to the control problem but it has to be completed from theoretical and experimental viewpoint by the geometric analysis of the observability properties of the system, related to the experimental sensors (force, joint angle) and online parameters estimation and aiming to design adaptative optimal controllers.

REFERENCES

[1] A.A. Agrachëv and R.V. Gamkrelidze, Symplectic geometry for optimal control, *Nonlinear controllability and optimal control*, Monogr. Textbooks Pure Appl. Math., Dekker, New York **133** 1990, 263–277

[2] T. Bakir, B. Bonnard B. and S. Othman, Predictive control based on nonlinear observer for muscular force and fatigue model, *2018 Annual American Control Conference (ACC)*, Milwaukee, WI (2018) 2157–2162.

[3] T. Bakir, B. Bonnard B. and J. Rouot, A case study of optimal input-output system with sampled-data control: Ding et al. force and fatigue muscular control model. *Netw. Hetero. Media*, **14** no.1 (2019), 79–100

[4] T. Bakir, B. Bonnard B., L. Bourdin and J. Rouot, Pontryagin-type conditions for optimal muscular force response to functional electrical stimulations. *J. Optim. Theory Appl.*, **184** (2020), 581–602.

[5] T. Bakir, B. Bonnard B., L. Bourdin and J. Rouot, Direct and Indirect Methods to Optimize the Muscular Force Response to a Pulse Train of Electrical Stimulation, preprint, hal-02053566.

[6] G.A. Bliss, Lectures on the calculus of variations, *University of Chicago Press*, Chicago, Ill., 1946 ix+296

[7] B. Bonnard and I. Kupka, Generic properties of singular trajectories, *Ann. Inst. H. Poincaré Anal. Non Linéaire*, **14** no.2 (1997), 167–186

[8] B. Bonnard and M. Chyba, Singular trajectories and their role in control theory, *Mathématiques & Applications (Berlin) [Mathematics & Applications]*, Springer-Verlag, Berlin, **40** 2003, xvi+357

[9] U. Boscain and B. Piccoli, Optimal syntheses for control systems on 2-D manifolds, *Mathématiques & Applications (Berlin) [Mathematics & Applications]*, **43** 2004, xiv+261

[10] N. Bourbaki, Lie groups and Lie algebras. Chapters 4–6, *Elements of Mathematics (Berlin)*, Springer-Verlag, Berlin, 2002, xii+300

[11] L. Bourdin and E. Trélat, Optimal sampled-data control, and generalizations on time scales, *Math. Cont. Related Fields*, **6** (2016), 53–94

[12] L. Bourdin and G. Dhar, Continuity/constancy of the Hamiltonian function in a Pontryagin maximum principle for optimal sampled-data control problems with free sampling times *Math. Control Signals Syst.* **31** (2019), 503-–544

[13] P. Brunovský, A classification of linear controllable systems, *Kybernetika (Prague)* **6** (1970), 173–188

[14] J.B. Caillau, O. Cots and J. Gergaud, Differential continuation for regular optimal control problems, *Optim. Methods Softw.*, **27** no.2 (2012), 177–196

[15] B.D. Doll, N.A. Kirsch and N. Sharma, Optimization of a Stimulation Train based on a Predictive Model of Muscle Force and Fatigue, *IFAC-PapersOnLine*, **48** no.20 (2015), 338–342

[16] J. Ding, A.S. Wexler and S.A. Binder-Macleod, Development of a mathematical model that predicts optimal muscle activation patterns by using brief trains, *J. Appl. Physiol.*, **88** (2000), 917–925

[17] J. Ding, A.S. Wexler and S.A. Binder-Macleod, A predictive fatigue model. I. Predicting the effect of stimulation frequency and pattern on fatigue, *IEEE Transactions on Neural Systems and Rehabilitation Engineering*, **10** no.1 (2002), 48–58

[18] J. Ding, A.S. Wexler and S.A. Binder-Macleod, A predictive fatigue model. II. Predicting the effect of resting times on fatigue, *IEEE Transactions on Neural Systems and Rehabilitation Engineering*, **10** no.1 (2002), 59–67

[19] R.V. Gamkrelidze, Discovery of the maximum principle, *J. Dynam. Control Systems*, **5** no.4 (1999), 437–451

[20] I.M. Gelfand and S.V. Fomin, Calculus of variations, *Prentice-Hall, Inc., Englewood Cliffs, N.J.*, 1963 vii+232

[21] R. Gesztelyi, J. Zsuga, A. Kemeny-Beke, B. Varga, B. Juhasz and A. Tosaki, The Hill equation and the origin of quantitative pharmacology, *Archive for history of exact sciences*, **66** no. 4 (2012), 427–438

[22] S. Helgason, Differential geometry, Lie groups, and symmetric spaces, *Graduate Studies in Mathematics*, **34** 2001, xxvi+641

[23] R. Hermann and A.J. Krener, Nonlinear controllability and observability, *IEEE Trans. Automatic Control* **AC-22** no.5 (1977), 728–740

[24] A. Isidori, Non-linear Control Systems, *3rd ed. Berlin, Germany: Springer-Verlag*, 1995

[25] A.N. Kolmogorov and S.V. Fomin, Introductory real analysis, *Prentice-Hall, Inc., Englewood Cliffs, N.J.*, 1970 xii+403

[26] E.B. Lee and L. Markus, Foundations of optimal control theory, 2nd edition, *Robert E. Kreiger Publishing Co., Inc., Melbourne* 1986, xii+576

[27] M.S. Marion, A.S. Wexler and M.L. Hull, Predicting fatigue during electrically stimulated non-isometric contractions, *Muscle & Nerve: Official Journal of the American Association of Electrodiagnostic Medicine*, **41** no.6 (2010), 857–867
[28] M.S. Marion, A.S. Wexler and M.L. Hull, Predicting non-isometric fatigue induced by electrical stimulation pulse trains as a function of pulse duration, *Journal of neuroengineering and rehabilitation*, **10** no.13 (2013)
[29] V. Renault, M. Thieullen and E. Trélat, Minimal time spiking in various ChR2-controlled neuron models, *J. Math. Biol.*, **76** no.3 (2018), 567–608
[30] H. Schättler and U. Ledzewicz, Geometric optimal control, *Interdisciplinary Applied Mathematics*, Theory, methods and examples, Springer, New York, 2012, xx+640
[31] H. Sussmann and V. Jurdjevic, Controllability of nonlinear systems, *J. Differential Equations* **12** (1972), 95–116
[32] R. Vinter, Optimal control, *Systems & Control: Foundations & Applications*, Birkhäuser Boston, Inc., Boston (2000).

TABLE 1. Numerical values for parameters of the Ding et al. model.

Variable	Value	Unit	Variable	Value	Unit
τ_c	20×10^{-3}	s	τ_{fat}	127	s
A_{rest}	3.009	$\mathrm{kN\,s^{-1}}$	$K_{m,rest}$	1.03×10^{-1}	
$\tau_{1,rest}$	5.1×10^{-2}	s	τ_2	1.24×10^{-1}	s
α_A	-4×10^{-1}	$\mathrm{s^{-2}}$	α_{K_m}	1.9×10^{-2}	$\mathrm{s^{-1}\,kN^{-1}}$
α_{τ_1}	2.1×10^{-2}	$\mathrm{kN^{-1}}$	R_0	2	

TABLE 2. Numerical values for parameters of the Marion et al. model.

Variable	Value	Unit	Variable	Value	Unit
F_{load}	45.4	N	F_M	247.5	N
τ_c	20×10^{-3}	s	τ_{fat}	99.4	s
$A_{90,0}$	2100	$\mathrm{N\,s^{-1}}$	$K_{m,0}$	3.52×10^{-1}	
$\tau_{1,0}$	3.61×10^{-2}	s	τ_2	5.21×10^{-2}	s
a	4.49×10^{-4}	$\mathrm{deg^{-2}}$	b	3.44×10^{-2}	$\mathrm{deg^{-1}}$
v_1	3.71×10^{-1}	$\mathrm{N\,deg^{-2}}$	v_2	2.29×10^{-2}	$\mathrm{deg^{-1}}$
$\ell = L/I$	9.85	$\mathrm{kg\,m^{-1}}$	α_A	-4.02×10^{-1}	$\mathrm{s^{-2}}$
α_{K_m}	1.36×10^{-5}	$\mathrm{s^{-1}\,N^{-1}}$	α_{τ_1}	2.93×10^{-5}	$\mathrm{N^{-1}}$
β_{τ_1}	8.54×10^{-7}	$\mathrm{s\,deg^{-1}\,N^{-1}}$	R_0	1.143	
β_{90}	0	$\mathrm{deg^{-1}\,s^{-1}}$	β_{K_m}	0	$\mathrm{deg^{-1}\,N^{-1}}$

Received xxxx 20xx; revised xxxx 20xx.

E-mail address: bernard.bonnard@u-bourgogne.fr
E-mail address: jeremy.rouot@grenoble-inp.org